Preprint of the paper:
Blocken B, Roels S, Carmeliet J. 2004. Modification of pedestrian wind comfort in the Silvertop Tower passages by an automatic control system. Journal of Wind Engineering and Industrial Aerodynamics 92(10): 849-873. © Elsevier 2004

Modification of pedestrian wind comfort in the Silvertop Tower passages by an automatic control system

Bert Blocken[*] [a], Staf Roels [a], Jan Carmeliet [a,b]

(a) Laboratory of Building Physics, Department of Civil Engineering, Katholieke Universiteit Leuven, Kasteelpark Arenberg 51, 3001 Leuven, Belgium
(b) Building Physics Group, Faculty of Building and Architecture, Technical University Eindhoven, P.O. box 513, 5600 MB Eindhoven, The Netherlands

Abstract

The Silvertop Towers project is a comprehensive redevelopment project of three high-rise residential buildings in the city of Antwerp (Flanders, Belgium). As part of this project, pedestrian passages will be constructed through each of the towers to improve the accessibility and to increase social control on the site. Experience, wind tunnel modeling and numerical modeling have indicated that wind conditions in passages are often unfavorable. This paper presents the assessment of wind climate and especially the study that has been performed to modify the wind climate in the passages of the Silvertop Towers. The assessment of wind climate is conducted with the aid of numerical modeling with CFD (Computational Fluid Dynamics). The wind climate is assessed to be highly unacceptable. Remedial action is imperative. Various traditional remedial measures to improve the wind climate are contemplated. These solutions either provide an insufficient improvement of wind climate or conflict with the envisaged architectural design. Therefore a rather unconventional solution has been selected. We have designed and analyzed an automatic control system to modify the wind climate in the passages. The actuators of the system are sliding doors that are mounted at both ends of the passage. The opening and closing of the doors is controlled by a decision algorithm based on local wind measurements. At least one of the doors will be closed when the control system senses that the threshold wind speed in the passage is exceeded. The control system will ensure an adequate wind climate without conflicting with the original architectural design. The passages are estimated to be opened for about 50 to 70% of the time. Estimates for the fraction of time that door control is imperfect (doors are closed instead of open and vice versa) are also given.

Keywords: Automatic control system; Pedestrian wind comfort; Numerical simulation; Wind climate assessment; Wind climate modification

1. Introduction

The Silvertop Towers are a group of three high-rise (60 m) residential buildings located in the south of Antwerp (Flanders, Belgium) near the Kiel Park (Figure 1). The towers were built in 1960. The decline of the towers and the neighborhood has urged the housing department to initiate a comprehensive redevelopment project. An architectural contest was organized. The new design had to meet several specific criteria: (1) to increase the accessibility of the towers

[*] Corresponding author: Bert Blocken, Laboratory of Building Physics, K.U.Leuven, Kasteelpark Arenberg 51, 3001 Leuven, Belgium. Tel.: +32 (0) 16-321345 - Fax: +32 (0) 16-321980
E-mail address: bert.blocken@bwk.kuleuven.ac.be

and the site, (2) to turn the site into a mobility node connecting nearby roads, parks, shops, tram stop and South Antwerp railway station, and (3) to increase public safety by social control (through sight). The latter was given high priority by the jury. In the contest winning design, pedestrian passages are constructed through each of the towers with the main intention to increase the accessibility of the towers and to increase social control. The tower entrances are situated in the passages, which are also part of a new walk-way that goes through the towers. These aspects also answer to the question of local police to increase social control and improve inspection by the policeman on the beat. The present paper will focus on the passages. Since they are the main point of the design, a favorable wind climate is imperative. The current authors were asked to assess the wind climate in the passages and, if needed, to suggest modifications restricted by the original design requirements.

The procedure for the assessment of wind climate comprises the combination of statistical meteorological data, aerodynamic information and a comfort criterion. Aerodynamic information is needed to transform the statistical meteorological data from the weather station to the building site where the wind climate is to be assessed. Once this link is established providing us with the wind statistics at the location of interest, a comfort criterion is used to judge local wind climate. The aerodynamic information (i.e. the wind flow conditions around the building) will partly be obtained by numerical (CFD) modeling. The modeling effort is supported by the sensitivity analysis and by the comparison of numerical and wind tunnel results performed in a recent research report [1].

Based on the outcome of the wind climate assessment, remedial action may be necessary. Previous papers and reports dealing with remedial measures have focused on structural improvements such as screens and fences, canopies, balconies and podium shaped extensions [2-11] or on the use of vegetation to improve wind climate [6,8]. To the knowledge of the current authors, up to now, no engineering solutions based on automatic control systems have been investigated or applied in this field. The development and analysis of such a control system to modify the wind climate, based on local wind measurements, is the main issue in the present paper.

The paper starts with some comments on the method that will be used for wind climate assessment in general and for the analysis of the automatic control system in particular (section 2). Section 3 describes the buildings, site and terrain. In section 4 the wind flow is numerically modeled. The assessment of the wind climate is performed in section 5. Remedial measures including the design and analysis of the automatic control system are dealt with in section 6. Section 7 comprises a discussion on - among others - the accuracy and reliability of the control system.

2. Some comments on the method for wind climate assessment

The method for the assessment of wind climate is well described in the literature (e.g. [11]). However, some specific features that are used in the present paper are addressed in this section: (1) The definition of the reference wind speed used. (2) The choice of the comfort criterion. (3) The determination of the standard deviation of the turbulent fluctuations σ_u. (4) The modification of the wind comfort criterion to take into account calculation errors. (5) The relationship between the amplification factor γ and the threshold exceedence probability P that will be used not only for the assessment of wind climate but also - and especially - for the analysis of the automatic control system.

(1) The aerodynamic information is comprised in the wind amplification factor γ that can be split into contributions from different spatial scales ([11]): a design related contribution (U/U_0) or local amplification factor and a terrain related contribution (U_0/U_{pot}):

$$\gamma = \frac{U}{U_{pot}} = \frac{U}{U_0} \cdot \frac{U_0}{U_{pot}} \quad (1)$$

where U_{pot} is the potential wind speed. The reference wind speed U_0 that is introduced here will be taken as the value that would occur at the location of interest (at pedestrian height = 1.75 m) if the buildings were absent. This definition is represented in Figure 2. With this choice, the local amplification factor U/U_0 directly indicates the amplification of wind speed due to the presence of the tower buildings. It will be determined by numerical modeling (CFD). The terrain related contribution U_0/U_{pot} takes into account the effect of the differences between the terrain roughness of the meteorological site, the city terrain surrounding the building site and the building site itself. It will be determined in section 5.

(2) The wind comfort criterion selected by Bottema [12] from his extensive comparison work will be used:

$$U_e = U + \sigma_u < 6 \text{ m/s} \quad (2)$$

$$P_{max} = 15\,\% \quad (3)$$

where U_e is the effective wind speed, U the mean wind speed, σ_u represents the turbulent fluctuations of the wind speed and P_{max} is the maximum allowed exceedence probability in time for the discomfort threshold or the allowed "discomfort probability" (15% for walking).

(3) σ_u in Eq. (2) will be taken equal to 2.4 u* ([13]), where u* is the friction velocity at the meteorological station. For $U \approx 6$ m/s and assuming the log law with $z_0 = 0.03$ m (grass covered plain), an u* is obtained that yields $\sigma_u \approx 1$ m/s. According to Bottema [11,14], pedestrian level σ_u is approximately constant and σ_u at the building site can be assumed equal to σ_u at the meteorological site. The threshold value applied to the mean wind speed U only is therefore about 5 m/s (Eq. 2).

(4) Recent research has provided information about the way that wind comfort criteria should be adapted to account for errors in the calculation of the total amplification factor γ. Information about errors in γ has been provided by Bottema [11], Willemsen and Wisse [15] and de Wit et al. [16]. The error in γ causes a standard error in the calculated probability P that the local wind speed exceeds a threshold value. An estimate for this error is $\delta P = 3\%$ for a threshold wind speed $U_{THR} = 5$ m/s [15]. From this estimate and assuming a normal distribution for the error in P and in order to get a 95% confidence level, a corrected value for the maximum allowed discomfort probability is obtained (Eq. 4). This corrected, more stringent value will be used in the following.

$$P_{max,cor} = P_{max} - (1.6 \cdot 3)\,\% = 10\,\% \quad (4)$$

(5) For a given discomfort threshold (Eq. 2) and given wind climate statistics, the relationship between γ_θ and the discomfort probability P_θ for each wind direction θ can be obtained. This relationship is briefly derived below because it will provide the basis, not only for the assessment of the wind climate but especially for the analysis of the automatic control system that will be presented later. The discomfort probability P_θ is the percentage of time that the discomfort threshold is exceeded for wind from direction θ. For calculating exceedence probabilities the Weibull distribution can be used:

$$P_\theta\left(U_{pot} > U_{THR,pot}\right) = 100 \cdot A(\theta) \exp\left[-\left(\frac{U_{THR,pot}}{c(\theta)}\right)^{k(\theta)}\right] \quad (5)$$

where $U_{THR,pot}$ is a given threshold for the potential wind speed, $P_\theta(U_{pot}>U_{THR,pot})$ is the probability of exceedence of $U_{THR,pot}$ by U_{pot} during wind direction θ, and A(θ), c(θ) and k(θ) are the Weibull parameters, respectively denoting: probability for wind direction θ, velocity scale for wind direction θ (m/s), shape parameter for wind direction θ. The Weibull parameters are determined by fitting Eq. (5) to statistical meteorological data. Eq. (5) applies to the potential wind speed. Our interest however is in the exceedence of the criterion wind speed threshold value U_{THR} = 5 m/s by the local wind speed U. Eq. (5) applying to potential wind speed must therefore be converted to an equation applying to local wind speed using the conversion factor γ_θ. As requirement (6) equals requirement (7), the exceedence probability of U_{THR} by the local wind speed U is given by Eq. (8). It provides the relationship between γ_θ and P_θ.

$$U < U_{THR} \quad (6)$$

$$U_{pot} < \frac{U_{THR}}{\gamma_\theta} = U_{THR,pot} \quad (7)$$

$$P_\theta = P_\theta\left(U > U_{THR}\right) = 100 \cdot A(\theta) \exp\left[-\left(\frac{U_{THR}}{\gamma_\theta \cdot c(\theta)}\right)^{k(\theta)}\right] \quad (8)$$

3. Description of building, site and terrain

The Silvertop Towers are situated in the south part of Antwerp. From north (0°) to approximately south-west (240°) the site is surrounded by urban terrain for a distance of more than 5 kilometers. From south-west to north, fetch is over rural terrain for some tens of kilometers. The building site is a localized smooth area within the terrain. The situation is similar to that represented in Figure 2a. Figure 3a illustrates the site of the Silvertop Towers (new design). Each tower is about 60 m high and north-south oriented. Towers 1 and 2 comprise three cross-shaped modules, tower 3 is made up of two such modules. Each module has a maximum width and length of 20 m. Low-rise buildings of 5 m height – called 'the finlets' - are constructed at the towers' base to house shops and the housing department offices. A small building of 5 m height called the 'energy building' is situated east of tower 3. South of the towers, an apartment building (LxBxH = 122x15x22 m³) and a concentration of house blocks of about 8 m high are situated. There are no other buildings within at least a 300 meter radius around the towers. Other high-rise buildings are at least 3 km away. Through-passages are constructed under each of the towers with building entrances in the passages (Figure 3b). A canopy divides each passage into two parts, further referred to as 'upper passage' and 'lower passage'. The lower passage has dimensions LxBxH = 13.5x4.2x3 m³. The upper passage has dimensions LxBxH = 6.5x4.2x1.6 m³ and has no specific function in the design. Note that the specific configuration of the building causes both passages to have a different length (Figure 3b).

4. Numerical modeling of the wind flow

4.1. Numerical model and comparison with wind tunnel experiments

In order to provide guidance for the numerical modeling of the wind flow around and through the Silvertop Towers, first, sensitivity analyses for simple rectangular buildings with through-passages were conducted. Next, numerical results for simplified geometrical configurations were obtained and compared to available published wind tunnel data. For the details of this study, the reader is referred to ref. [1]. A few of the results will be given here. Figure 4 shows the basic geometry of the buildings that were studied. The wind flow has been modeled by solving the 3D Reynolds-Averaged Navier-Stokes equations with the commercial CFD code Fluent 5.4 [17]. Closure is obtained by using an improved version of the standard k-ε model: the realizable k-ε model developed by Shih et al. [18]. The term "realizable" refers to mathematical constraints on the normal stresses that are satisfied by the model: positivity of normal stresses and Schwarz inequality for shear stresses. The realizable k-ε model was shown to perform substantially better than the standard k-ε model [1]. Non-equilibrium wall functions instead of standard wall functions were employed in the calculations. The reason is their capability to partly account for the effects of pressure gradients and departure from equilibrium, which makes them more suitable for complex flows involving strong adverse pressure gradients, separation and recirculation. The equations are discretized using the control volume method. The numerical model was applied to examine the pedestrian wind conditions in through-passages for different building and passage dimensions and for different wind directions. The numerical results were compared with wind tunnel measurements provided by Wiren [5]. As an example, Figure 5a and b illustrate numerically and experimentally determined amplification factor values U/U_0 along the passage center line, at pedestrian height (2 m) and for a varying passage width (where U is the wind speed in the passage and U_0 is the wind speed at the same position with the building absent). Figure 5c shows maximum amplification factors in the passage at pedestrian height as a function of the building height. The sensitivity analysis and the comparison procedure as described in [1] have indicated that pedestrian wind conditions in passages through buildings with simple geometry can generally be modeled with an error of less than 10%, on condition that: (1) The blockage ratio is below 5% with the additional restriction that the width-to-height ratio of the domain is taken approximately equal to the width-to-height ratio of the building model. (2) Local mesh refinement is applied near the passage entrance and inside the passage, with tetrahedral control volumes having a mesh size of about 0.05λ, where λ is a parameter representing a characteristic dimension of the passage defined as $(b + h)/2$. (3) The realizable k-ε model is used. These guidelines have all been taken into account in the simulations described in the next section.

4.2. Model application

The model of Silvertop Towers, finlets, energy building, apartment building and house blocks is immersed in a boundary layer flow with a logarithmic mean wind speed profile. The steady-state wind flow pattern is calculated for 12 wind directions (clockwise from north = 0° at 30° increments). Roughness length "$z_{0,city}$" for the inflow is taken 1 m (urban terrain, 30° through 210°), 0.25 m (rural terrain, 270° through 330°) and 0.5 m (transition from rural to urban, 0° and 240°) according to the updated Davenport roughness classification [19]. Local $z_{0,loc}$ within a distance of 300 m from the towers is 0.03 m (level country, low vegetation, tarmac). Building roughness $z_{0,b}$ is taken 0.01 m. The dimensions of the computational domain are LxBxH = 900x700x190 m³. Solid blockage varies between 2 and 5% depending on the orientation of the model within the domain. It is noted that an appropriate width-to-height ratio of the domain has been obtained based on the model dimensions. Grid geometry and grid resolution are based on the findings of the sensitivity analysis; e.g. the size of the control volumes in the passage, near the passage entrance and on the faces of the canopy is taken about 0.05λ (0.15 m). An unstructured, tetrahedral grid with approximately 2.9×10^6 cells is obtained. The mesh on the west face of tower 1 is depicted in Figure 6. The second order discretization

scheme has been used for the convection terms of the governing equations (second order accuracy has always been used for the viscous terms). Turbulence property profiles (k and ε) that are in equilibrium with the upstream roughness length have been used as inlet conditions.

The results are presented as the local amplification factor U/U_0 at pedestrian height (1.75 m). Figure 7 displays a rose of U/U_0 values in the passage of tower 1. The represented values are the highest values found in the passage averaged over 1 m² horizontal area. Wind conditions in the passage appear to be strongly dependent on wind direction. This dependency is different for each tower and is most irregular for tower 1. As could be expected, wind directions perpendicular to the passage yield small amplification factors. Phenomena occurring for the other wind directions (for tower 1) can be explained focusing on wind directions 30 and 120°. Figure 8a illustrates contours of U/U_0 for wind direction 30° in a horizontal plane at 1.75 m height above ground. Figure 8b displays static pressure contours in the same plane. Figure 9 illustrates contours of U/U_0 for wind direction 120°. For 30°, north-easterly wind, the amplification factor is large (Figure 7, 8a). The main reason is the presence of the low-rise building (finlet) and canopy near the passage entrance of tower 1 that yield a local additional overpressure build-up (Figure 8b). This increases the pressure difference over the passage. For 120°, south-easterly wind, the wind amplification factor for tower 1 is small (Figure 7, 9). Again, the main reason is the presence of the finlet and canopy near the passage entrance that now have the adverse effect: flow separation occurs at the edge. This gives rise to a low-pressure zone in front of the passage entrance and reduces the pressure difference over the passage. Note that the pressure values in Figure 8b are not presented as dimensionless values. The absolute values presented here correspond to an inlet wind speed at 10 m height of U_{10} = 5 m/s.

5. Assessment of the wind climate in the passages

The situation for the transformation of the aerodynamic information has been schematically represented in Figure 2a. Statistical meteorological data (hourly values of potential wind speed U_{pot} and wind direction) are made available by the Royal Dutch Meteorological Institute (KNMI). The potential wind speed U_{pot} is the wind speed measured at 10 m height at an ideal meteorological station with an aerodynamic roughness length $z_{0,meteo}$ = 0.03 m. The data of the station of Eindhoven are selected for its proximity to Antwerp (70 kilometers). The data covers the period 1971 to 2000 and is transformed to the building site by means of the total wind amplification factor γ. U/U_0 has been calculated in section 4. U_0/U_{pot} is obtained by splitting the ratio into two factors:

$$\frac{U_0}{U_{pot}} = \frac{U_0}{U_{10}} \cdot \frac{U_{10}}{U_{pot}} \tag{9}$$

The first factor incorporates the influence of the sudden roughness change (development of the internal boundary layer - IBL) and of other occasional terrain irregularities that are present between the roughness change and the building location. It can be determined by numerical modeling of the situation represented in Figure 2b: the wind flow is modeled in a domain without the building models present. The second factor is obtained by combining the expression of the vertical wind speed profile by the logarithmic law (Eq. 10) and the formula derived by Simiu and Scanlan [20] (Eq. 11):

$$\frac{U_{10}}{U_{pot}} = \frac{U_{city}(z=10\,m)}{U_{meteo}(z=10\,m)} = \frac{u^*_{city}\cdot \ln\left(\frac{10\,m}{z_{0,city}}\right)}{u^*_{meteo}\cdot \ln\left(\frac{10\,m}{z_{0,meteo}}\right)} \quad (10)$$

$$\frac{u^*_{city}}{u^*_{meteo}} = \left(\frac{z_{0,city}}{z_{0,meteo}}\right)^{0.0706} \quad (11)$$

Following this procedure, separate values for the conversion factor γ_θ are obtained for each wind direction θ. From the knowledge of γ_θ, discomfort probabilities P_θ for each wind direction are obtained by using Eq. (8). The Weibull parameters in this equation are determined based on the Eindhoven meteorological data. The data has been found to fit the Weibull distribution well. Calculating and summing P_θ for all wind directions yields the total discomfort probability P which should not exceed $P_{max,cor}$ = 10 % (Eq. 4). This procedure yields P = 49.1%, 55.4% and 43.5% for tower 1, 2 and 3 respectively, all considerably exceeding the allowed $P_{max,cor}$ = 10%. Measures to improve the wind climate are imperative.

6. Modification of the wind climate in the passages

6.1. Options

Several options are contemplated: (1) elongation of the passages with tubes, (2) screens in the passages, (3) a revolving door in the passages and (4) sliding doors in the passages. The evaluation of each option is based on two criteria: (1) compatibility with the envisaged architectural design and (2) sufficient improvement of wind climate. The options are discussed in order of increasing compatibility with the envisaged design.

Tubes: The cause of the bad wind climate in the passages is pressure short-circuiting through the passage between wind (overpressure) and leeward (underpressure) side of the building. A possible solution is to decrease the pressure difference over the passage by extending it with airtight transparent tubes that end outside the over- and underpressure zones. Since the extent of these zones would easily give rise to long tubes and as this was not considered compatible with the envisaged design, this option was rejected.

Screens: Instead of reducing the pressure difference one can consider increasing the flow resistance in the passages with screens. Wind tunnel studies of the effect of different screen configurations in passages were carried out by Beranek [8]. It was found that: (1) Screens can significantly reduce the overall wind speed in the passage, however at the expense of local strong wind speed values near the screen edges. (2) For a significant reduction of wind speed, screens should cover more than 50–75% of the passage section, which is too much and – among others - conflicts with fire safety requirements.

Revolving door: Placing a four-wing revolving door in the passage has the advantage of a comfortable wind environment without actually closing the passage. Disadvantages however are: (1) The poor compatibility with the architectural features of the envisaged design. (2) The reduced transparency of the passages by the round shapes, conflicting with the “social control through sight” aspect. (3) The revolving door will always be an obstacle for pedestrians using the passage even in calm weather.

Sliding doors: The solution that is finally selected is to install sliding doors at both ends of the lower passage and to control the opening and closing of the doors based on local wind measurements. During unfavorable wind conditions, a comfortable wind environment is ensured when at least one of the doors is closed. During favorable wind conditions, the doors can remain opened. A double automatic control system is required: (1) A control system that

detects the occurrence of unfavorable or favorable wind conditions and respectively closes one of the doors or opens both doors. (2) An automatic control system that - during unfavorable wind conditions – senses the presence of pedestrians and opens one of the doors while the other one remains closed.

6.2. Automatic control system

6.2.1. Control system components

The geometry of the passage with sliding doors (when opened) is given in Figure 10. The second control system described above can be taken similar to the well-known control system used for existing automatic sliding or revolving door systems. The first control system is more complex, and it will be discussed next. The variable to be controlled is the wind speed in the lower passage. The variable to be measured by the sensor (anemometer) should be a wind speed that is related to the wind speed in the lower passage. It can obviously not be measured in the lower passage itself, as this will be closed for a certain percentage of the time. The most straightforward choice is to place the anemometer in the upper passage that is permanently opened and has no other function in the design (Figure 3b). The advantages of this choice are the limited distance between all control system components and the fact that the wind speed in the lower and in the upper passage are expected to be strongly related. The proposed open loop control system has the basic components given in Table 1. The setpoint results from the discomfort threshold for the mean wind speed: Eq. (2): $U_{THR} = U_{e,THR} - \sigma_u \approx 5$ m/s. The relationship between the measured variable and the controlled variable must be determined. Based on this relationship and the value of the measured variable, a value for the controlled variable is obtained. Based on the difference between the controlled variable value and the setpoint value, the controller will take control action. The following issues need to be addressed: (1) Position of the anemometer in the upper passage. (2) Relation between wind speed in upper and lower passage. (3) Measuring frequency of the anemometer and decision algorithm.

6.2.2. Position of the anemometer

The anemometer position is chosen based on the characteristics of the calculated flow field in the upper passage (Figure 11 and 12a, b). For well functioning of the automatic control system, it is essential that the anemometer be placed at a position where an adequate measurement of the upper passage wind speed can be made, i.e. not in regions with high wind speed gradients and/or regions of flow reversal.

(1) Choice of the vertical position. Figure 11: In the vertical plane, flow separates when entering the upper passage. The anemometer will be placed outside the recirculation region and at a position where wind speed gradients are low, i.e. at 0.6 m from the top face of the canopy (at 4 m height above ground level).
(2) Choice of the horizontal position. Figure 12a, b: In a horizontal plane through the upper passage at 4 m height above ground, wind speed gradients appear to be quite small, as opposed to those in the lower passage. Gradients remain small even if the approach flow direction is not parallel to the passage, as for tower 2 and 3 where the direction of the approach flow is disturbed due to the towers upstream. The anemometer will be positioned in the middle of the horizontal section of the upper passage (see Figure 10).

6.2.3. Relation between wind speed in upper and lower passage (sliding doors opened)

The fixed parts of the sliding doors in fact are screens in the passage and add flow resistance, resulting in a limited improvement in wind climate, as can be observed in Figure 12a. For the configuration with fixed sliding door parts (sliding doors open and upper passage open) and for the configuration with sliding doors closed (only upper passage open), new CFD calculations are conducted for all 12 wind direction classes. Amplification factors U/U_0 in the lower passage

and in the upper passage (at the anemometer position) are calculated and the wind climate is assessed again. Figure 13 illustrates the results for tower 1 as an U/U_0 rose giving: (1) U/U_0 in the lower passage (maximum averaged over 1m² at 1.75 m height). (2) U/U_0 in the upper passage (at anemometer position - doors are opened). (3) U/U_0 in the upper passage (at anemometer position - doors are closed). Comparing Figure 13 with Figure 7 illustrates the effect of the fixed sliding door parts: the amplification factors are decreased. Nevertheless uncomfortable conditions still exist for up to P = 39%, 37% and 27% for towers 1, 2 and 3 respectively. Figure 13 shows that the wind amplification factor in the upper passage is practically independent of the status of the doors. However, the ratio between the amplification factor in upper and lower passage is wind direction dependent (Figure 13). This dependency is most complex for tower 1. Part of it can be explained by the presence of the low-rise finlet near the passage entrance. As indicated earlier for 30° an additional overpressure is generated under the canopy as opposed to above it (Figure 8). This is also the case for 60, 300 and 330°. For 120 and 150°, flow separation gives rise to a lower pressure zone under the canopy (Figure 9). For tower 2 and 3, the low-rise finlet is located further from the passage entrance and as a result these effects are less important and the relation is more regular. Given the fact that the relation between wind speed in upper and lower passage is wind direction dependent, two options are available:

(1) The measured upper passage wind speed (measured variable) will be converted to the lower passage wind speed (controlled variable) using wind direction dependent correction factors. These factors can be calculated from Figure 13 by dividing U/U_0 in the lower passage by U/U_0 in the upper passage for each wind direction. However, this option requires measuring the (free field) wind direction, which is not possible in the upper passage. An additional measurement position outside the wind-flow pattern that is disturbed by the towers should be selected and the advantages of measuring in the upper passage are lost.
(2) The measured variable will be converted to the controlled variable using one single correction factor that is independent of wind direction. This way an *estimate* for the controlled variable will be obtained.

The latter option is selected. A first choice for the correction factor β will be based on Figure 13 (and the corresponding figures for the other two towers) where the difference in amplification factor U/U_0 between upper and lower passage is minimized using the weighted least squares method. The following expression is minimized:

$$\sum_{\theta} A(\theta)\left[\beta\left(\frac{U}{U_0}\right)_{upper} - \left(\frac{U}{U_0}\right)_{lower}\right]^2 \qquad (12)$$

where $A(\theta)$ is the probability for wind direction θ (Weibull parameter, see section 2), β is the correction factor, $(U/U_0)_{upper}$ is the amplification factor in the upper passage and $(U/U_0)_{lower}$ in the lower passage. This yields the following correction factors (index denotes tower number): β_1=0.81; β_2=0.88; β_3=0.76. Multiplying the measured value with these correction factors will sometimes yield an underestimation, sometimes an overestimation of the wind speed in the lower passage. E.g.: for 30° in the passage of tower 1, the wind speed in the lower passage is significantly underestimated. Subsequently, doors will be opened instead of closed for a certain percentage of time. In this period, the discomfort threshold in the passage is exceeded. The opposite holds for an overestimation. The probability (percentage of time) that the doors are closed (P_c), opened (P_o), opened instead of closed (P_{oc}) and closed instead of opened (P_{co}) can be calculated using the Weibull function (Eq. 13 to 16). Eq. 13 yields the probability of exceedence of the threshold, where the probability is calculated based on the actual amplification factor in the lower passage: $(U/U_0)_{lower}$. This is the (theoretically) exact value for

P_θ and the fraction of time that doors should actually be closed. Eq. 14 yields the probability of exceedence as estimated by the control system. This is the fraction of time that the doors will actually be closed by the control system (for the current wind direction). The percentages P_c and P_o are then given by Eq. (15). The percentage P_{co} (Eq. 16) is the time that the doors should be opened (according to Eq. 13) but remain closed due to imperfect control. P_{oc} is calculated in the same way.

$$P_\theta = 100 \cdot A(\theta) \exp\left[-\left(\frac{U_{THR}}{\left(\frac{U}{U_0}\right)_{lower} \cdot \frac{U_0}{U_{pot}} \cdot c(\theta)} \right)^{k(\theta)} \right] \tag{13}$$

$$P_\theta^{est} = 100 \cdot A(\theta) \exp\left[-\left(\frac{U_{THR}}{\beta\left(\frac{U}{U_0}\right)_{upper} \cdot \frac{U_0}{U_{pot}} \cdot c(\theta)} \right)^{k(\theta)} \right] \tag{14}$$

$$P_c = \sum_\theta P_\theta^{est} \quad ; \quad P_o = 100 - P_c \tag{15}$$

$$P_{co} = \sum_{P_\theta^{est} - P_\theta \rangle 0} \left[P_\theta^{est} - P_\theta \right] \quad ; \quad P_{oc} = \sum_{P_\theta - P_\theta^{est} \rangle 0} \left[P_\theta - P_\theta^{est} \right] \tag{16}$$

Table 2 shows the percentages P_{co} and P_{oc} for each of the towers and for each wind direction. It is noted that using the above formulae implies the assumption of an instantaneous control system (no deadtime). Deadtime is the time between an actual change in lower passage wind speed and when the control system responds to this change. Its implications will be discussed in the next section. Note that when we consider the passages equipped with the control system, the comfort criterion (Eq. 2 and 3) must be changed (although it inherently remains the same): the probability of exceedence P_{oc} has now become the discomfort probability, which should not be more than $P_{max,cor} = 10\%$.

Instead of minimizing Eq. (12), it may seem more sensible to minimize the sum of the percentages of imperfect control ($P_{oc} + P_{co}$). Moreover, P_{oc} (discomfort probability) could be considered more important than P_{co}, hence weighting factors could be applied (Eq. 17).

$$W_{oc} \cdot P_{oc} + W_{co} \cdot P_{co} \tag{17}$$

Table 3 yields door status time percentages for five different cases (different sets of correction factors):

(1) Case 1 implies a "perfect" control system: wind direction dependent correction factors are used. In this case, the percentage of time that the doors are closed equals the values of the discomfort probability that were given at the beginning of this section (39, 37, 27%), while the actual discomfort probability (P_{oc}) is zero.

The next cases use a single correction factor that is independent of the wind direction.

(2) Case 2 employs the correction factors determined by the weighted least squares method (WLSM) (minimize Eq. 12). Imperfect control ($P_{oc} + P_{co}$) occurs most frequently for tower

1, because of the irregular relation between U/U_0 in upper and lower passage (Figure 13). For the other two towers, the relation is more regular and there is less imperfect control.

(3) In case 3, correction factors have been determined to yield a zero discomfort probability (P_{oc} = 0%). As a result, P_{co} and P_c are rather large.

(4) Case 4 uses the correction factors determined by minimizing the percentage of imperfect control (MIC), with both weighting factors equal to one and with the restriction that P_{oc} must not exceed $P_{max,cor}$ = 10%.

(5) Case 5 is identical to case 4 but with a larger weight for P_{oc} than for P_{co}.

Note that the percentage P_c comprises the percentage P_{co} and that in each case and for each tower, Eq. (18) holds:

$$P_c - P_{co} + P_{oc} = \sum_{\theta} P_{\theta} \tag{18}$$

where the right hand side of the equation refers to the fraction of time that the doors would be closed if the control system were perfect. All cases satisfy the comfort requirement ($P_{oc} \leq 10\%$). As opposed to case 3, cases 2, 4 and 5 offer the advantage of limited percentages of imperfect control. At first sight, each of these three cases appears to be a suitable choice. However, the values in Table 3 assume that the control system acts instantaneously, which is practically impossible. This will be addressed in the next section.

6.2.4. Measuring frequency of the anemometer and decision algorithm

Different options are available here. A detailed evaluation of deadtime and choice of decision algorithm would require higher frequency statistical data (less than hourly). As these are not available, the measuring frequency of the anemometer and the decision algorithm are based on the wind speed power spectrum of Van der Hoven [21]. The power spectrum shows a "spectral gap" for periods of 10 minutes to an hour where wind speed is approximately stationary. Selecting an averaging period for wind speed measurements of 10 minutes to an hour will yield stable averaged values. A simple decision algorithm might be: (1) Measure wind speed on a 10-minute basis. (2) Multiply measured value with correction factor to obtain estimate of controlled variable value. (3) IF estimate is smaller than the setpoint value: open doors or keep doors open, ELSE close one of the doors or keep doors closed. (4) Repeat steps 1 to 3 for each 10-minute interval. With this algorithm, control will always be lagging 10 minutes behind (deadtime). As a result, the fraction of time of imperfect control will increase and the percentages in Table 3 will change. Since time control is situated in the spectral gap, changes are expected to be limited. Nevertheless, with this in mind and recalling Table 3 and the threshold value of 10%, case 2 or 5 might rather be chosen than case 4.

7. Discussion

Wind climate assessment is a complex matter and it is prone to errors. The automatic wind climate control system that has been designed and analyzed in this paper directly results from the wind flow calculations and the wind climate assessment. Therefore, special care has been taken to limit errors and to take into account the effect of errors in the analysis in several ways:

- The numerical simulation. Up to now, there are no generally accepted guidelines for the application and for the accuracy of CFD in wind engineering [22,23]. For this reason, a sensitivity analysis on simple rectangular building configurations and a comparison of the CFD results with wind tunnel experiments have been performed prior to the analysis in the present paper [1]. From these studies, guidelines for the present more complex simulation

were extracted (grid size in and near the passage, the importance of local grid refinement, use of the realizable k-ε model, etc).

- The choice of the comfort criterion. It has been selected from an extensive comparison procedure [12] and is one of the very few that have an experimental basis.
- The maximum allowed exceedence probability of the discomfort threshold in the criterion has been lowered to take into account errors associated with the total wind amplification factor γ [15].

It is recognized that, despite these efforts, errors will be present and that therefore the actual performance of the wind climate control system will show deviations from the calculated performance. It is also recognized that adjusting the control system setpoint might be necessary if experience and local inquiry after building completion should indicate that the comfort criterion does not accurately represents the pedestrian perceptions. In spite of these remarks, it is believed that the design and analysis of the automatic control system is the best solution for the problem: the wind climate in the passages is considerably improved and conflicts with the original architectural design have been avoided. Research in the near future will focus on the evaluation of the automatic control system based on a full-scale measurement program in the passages.

8. Conclusions

As part of a comprehensive redevelopment project, passages will be constructed through the Silvertop Towers in Antwerp. The pedestrian wind environment in the passages was assessed to be highly unfavorable. Traditional remedial measures could not provide a satisfactory solution. Therefore in the present paper an automatic control system has been designed and analyzed to modify the wind climate in the passages. The actuators are sliding doors that are mounted at both ends of the passage and that are controlled based on local wind measurements. The measurements are performed in upper through-passages above the passage canopies. The control system is estimated to leave doors open for about 50 to 70% of the time. The fraction of time that door control is imperfect (doors are closed instead of open and vice versa) has been limited.

Acknowledgements

This research is funded by the government of Flanders. As a Flemish government institution, IWT (= Institute for the Promotion of Innovation by Science and Technology in Flanders; Instituut voor de aanmoediging van Innovatie door Wetenschap en Technologie in Vlaanderen) supports and stimulates industrial research and technology transfer in the Flemish industry. Their contribution is gratefully acknowledged. The Royal Dutch Meteorological Institute is acknowledged for providing the meteorological data that was used in this research.

Appendix: list of symbols

A, c, k	Weibull parameters (-), (ms^{-1}), (-)
B	building width (m)
b	passage width (m)
H	building height (m)
h	passage height (m)
k	turbulent kinetic energy (m^2s^{-2})
L	building length (m)
P	threshold exceedence probability (for all wind directions) (% time)
P_c	probability that doors of control system are closed (% time)

P_{co}	probability that doors of control system are closed instead of opened (% time)
P_o	probability that doors of control system are opened (% time)
P_{oc}	probability that doors of control system are opened instead of closed (% time)
P_θ	exceedence probability for wind direction θ (% time) (actual value)
P_θ^{est}	exceedence probability for wind direction θ (value as estimated by control system)
P_{max}	maximum allowed exceedence probability (% time)
$P_{max,cor}$	maximum allowed exceedence probability, corrected value (% time)
u*	friction velocity (ms^{-1})
U	local wind speed at pedestrian height (buildings present) (ms^{-1})
U_0	reference wind speed – local wind speed at pedestrian height (buildings absent) (ms^{-1})
U_{10}	inlet wind speed in computational domain at 10 m height (ms^{-1})
U(z)	wind speed at height z (ms^{-1})
U_e	effective wind speed (ms^{-1})
U_M	maximum value of U along passage center line (ms^{-1})
U_{pot}	potential wind speed (ms^{-1})
U_{THR}	threshold value for the local wind speed U (ms^{-1})
$U_{THR,pot}$	threshold value for the potential wind speed U_{pot} (ms^{-1})
W_{co}, W_{oc}	weighting factors for P_{co}, P_{oc} respectively (-)
x, z	length and height co-ordinate (m)
$z_{0,b}$	building roughness (m)
$z_{0,city}$	aerodynamic roughness length for the city terrain (m)
$z_{0,loc}$	local terrain roughness (m)
$z_{0,meteo}$	aerodynamic roughness length for the terrain of the meteorological site (m)
δP	error in calculated exceedence probability (% time)
β	correction factor for sliding door control system (-)
ε	turbulence dissipation rate (m^2s^{-3})
θ	wind direction (clockwise from north, north = 0°)
γ	total wind amplification factor (-)
κ	von Karman constant (≈ 0.4)
σ_u	standard deviation of wind speed (ms^{-1})

References

[1] B. Blocken, S. Roels, J. Carmeliet, Pedestrian wind conditions in passages through buildings - Part 1. Numerical modeling, sensitivity analysis and experimental verification, Research report, Laboratory of Building Physics, Catholic University of Leuven, 99 p, 2003.

[2] M. O'Hare, R.E. Kronauer, Fence designs to keep wind from being a nuisance, in: Archit. Rec. (July 1969), 1969. pp. 151-156.

[3] A.F.E. Wise, Wind effects due to groups of buildings, in: Proceedings of the Royal Society Symposium Architectural Aerodynamics, London, February 26-27, 1970.

[4] V.K. Sharan, Wind comfort and wind shelter, in: Proceedings of the Symposium on External Flows, University of Bristol, 1972.

[5] B.G. Wiren, A wind tunnel study of wind velocities in passages between and through buildings, in: Proceedings of the 4th International Conference on Wind Effects on Buildings and Structures, (Heathrow 1975), 1975. pp. 465-475.

[6] N. Isyumov, A.G. Davenport, The ground level wind environment in built-up areas, in: Proceedings of the 4th International Conference on Wind Effects on Buildings and Structures, (Heathrow 1975), 1975. pp. 403-422.

[7] P. Merati, R. Wigeland, R., H. Nagib, Control of adverse wind near buildings, in: Proceedings of the American Society of Civil Engineers, 108, 5, 1982. pp. 509-521.

[8] W.J. Beranek, Beperken van windhinder om gebouwen, deel 2, (in Dutch) Stichting Bouwresearch no. 90, Kluwer Technische Boeken BV, Deventer, 149 p + 89 p, 1982.

[9] H.J. Gerhardt, C. Kramer, C. Wind shelters at the entrance of large buildings – case studies, in: Proceedings of the 6th Colloquium on Industrial Aerodynamics, Fluid Mechanics Laboratory, Department of Aeronautics, Fachhochschule, (Aachen, 1985), 1985.
[10] N.J. Jamieson, P. Carpenter, P.D. Cenek, The effect of architectural detailing on pedestrian level wind speeds, J. Wind Eng. Ind. Aerodyn. 41-44 (1992) 2301-2312.
[11] M. Bottema, Wind climate and urban geometry. Ph.D. thesis FAGO, Technical University of Eindhoven, 212 p, 1993.
[12] M. Bottema, A method for optimisation of wind discomfort criteria, Build. Environ. 35 (2000) 1-18.
[13] H.A. Panofsky, J.A. Dutton, Atmospheric turbulence. John Wiley and sons, New York, 397 p, 1984.
[14] M. Bottema, J.A. Leene, J.A. Wisse, Towards forecasting of wind comfort, J. Wind Eng. Ind. Aerodyn. 41-44 (1992) 2365-2376.
[15] E. Willemsen, J.A. Wisse, Accuracy of assessment of wind speed in the built environment, J. Wind Eng. Ind. Aerodyn. 90 (2002) 1183-1190.
[16] M.H. de Wit, T. Stathopoulos, J.A. Wisse, Airport wind speeds used for the design in urban environments: the Eindhoven case, J. Wind Eng. Ind. Aerodyn. 90 (2002) 1289-1298.
[17] Fluent Inc., Fluent 5 User's Guide, 4 vols, 1998.
[18] T.-H. Shih, W.W. Liou, A. Shabbir, J. Zhu, A new k-ε eddy-viscosity model for high Reynolds number turbulent flows – model development and validation, Comput. Fluids 24, 3 (1995) 227-238.
[19] J. Wieringa, Updating the Davenport roughness classification, J. Wind Eng. Ind. Aerodyn. 41-44 (1992) 357-368.
[20] E. Simiu, R.H. Scanlan, Wind effects on structures. An introduction to wind engineering. Second Edition, John Wiley and Sons, New York, 589 p, 1986.
[21] I. Van der Hoven, Power spectrum of horizontal wind speed in the frequency range from 0.0007 to 900 cycles per hour. J. Meteorol. 14 (1957) 160-164.
[22] J.A. Wisse, H.W. Krüs, E. Willemsen, Wind comfort assessment by CFD – context and requirements, in: G. Augusti, C. Borri, C. Sacré, (Eds.), Impact of Wind and Storm on City Life and Built Environment, Workshop proceedings, Cost Action C14 (Nantes, 2002), 2002. pp. 154-163.
[23] S. Murakami, Setting the scene: CFD and symposium overview, Wind Struct. 3 (2002) 83-99.

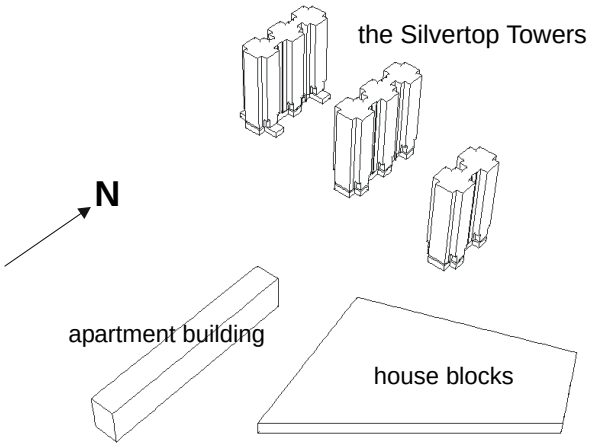

Figure 1

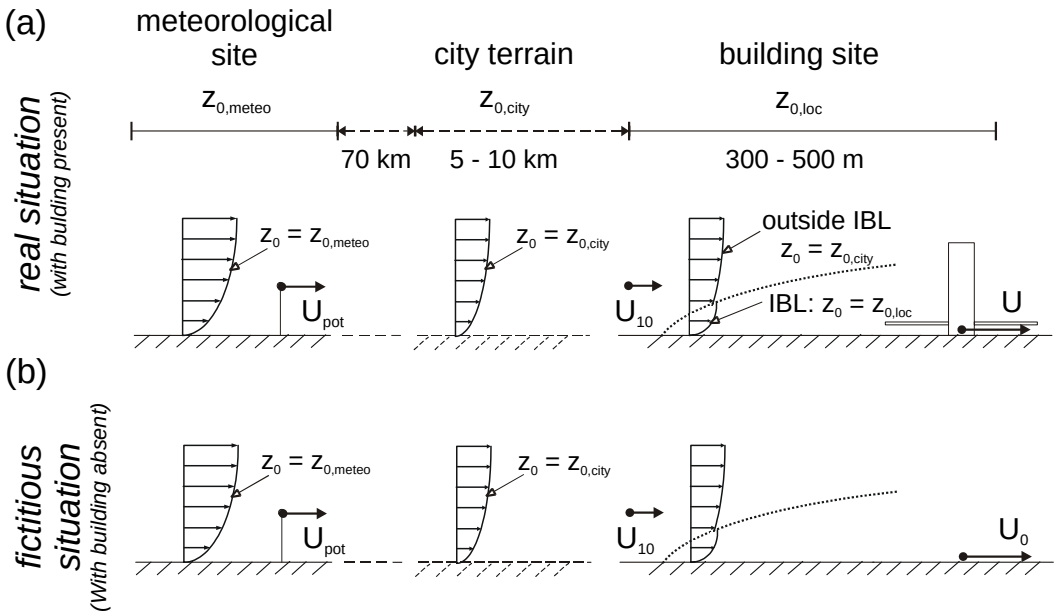
(a)
meteorological site
city terrain
building site
real situation
(with bulding present)
$z_{0,meteo}$
$z_{0,city}$
$z_{0,loc}$
70 km
5 - 10 km
300 - 500 m
$z_0 = z_{0,meteo}$
U_{pot}
$z_0 = z_{0,city}$
outside IBL
$z_0 = z_{0,city}$
IBL: $z_0 = z_{0,loc}$
U_{10}
U
(b)
fictitious situation
(With building absent)
$z_0 = z_{0,meteo}$
U_{pot}
$z_0 = z_{0,city}$
U_{10}
U_0

Figure 2

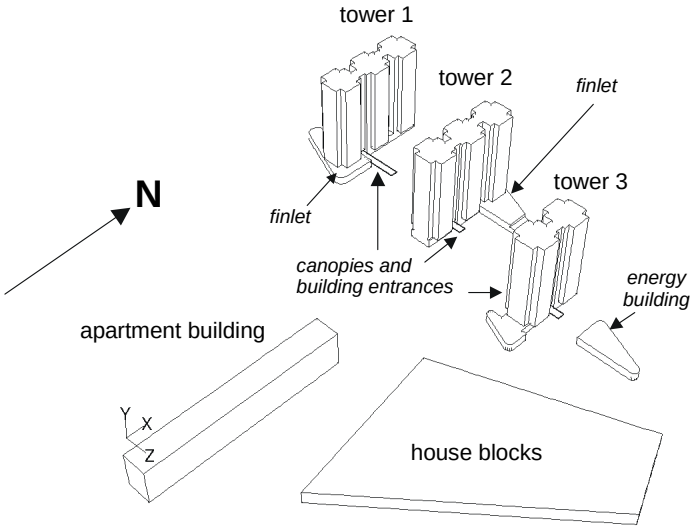

Figure 3a

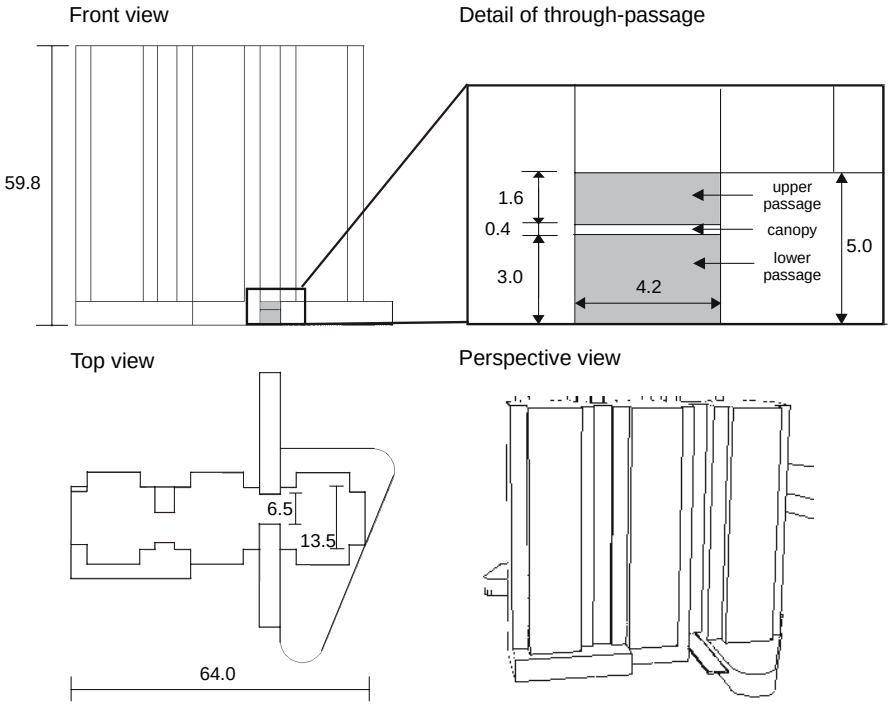

Figure 3b

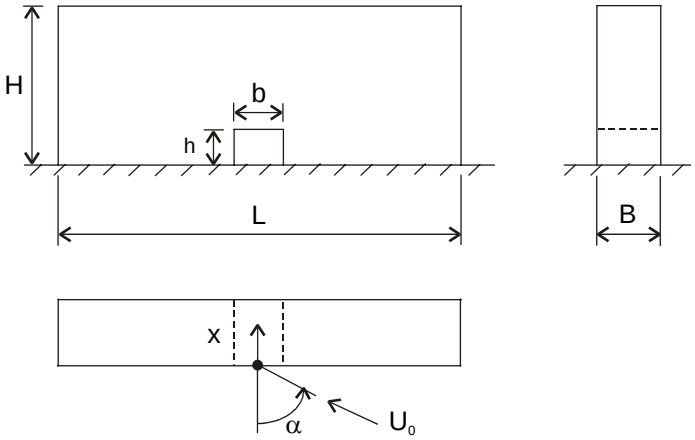

Figure 4

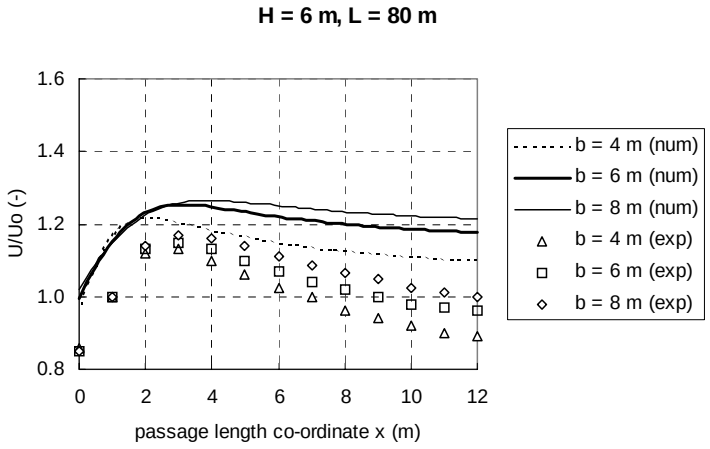

Figure 5a

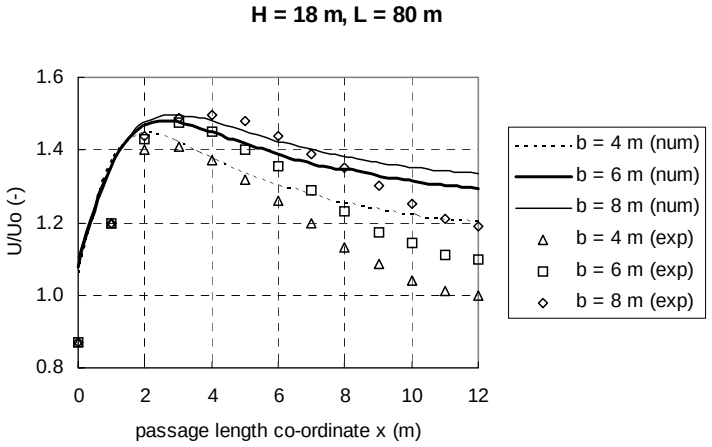

Figure 5b

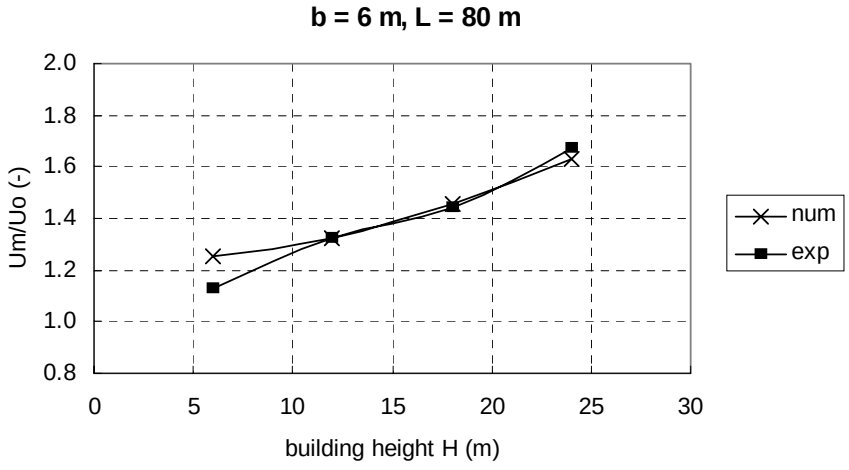

Figure 5c

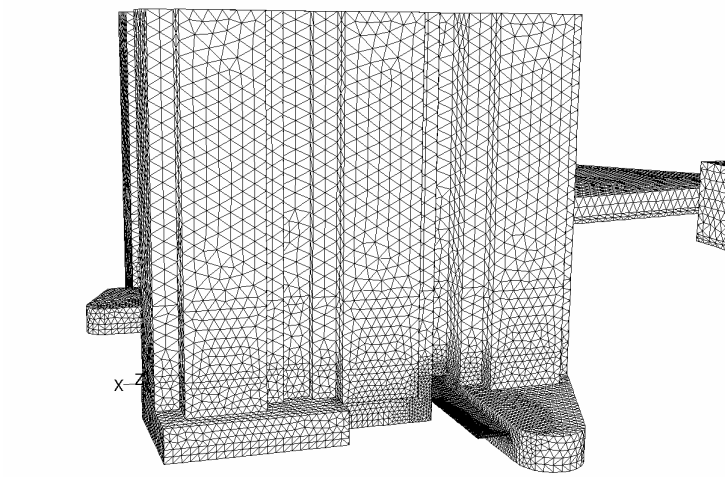

Figure 6

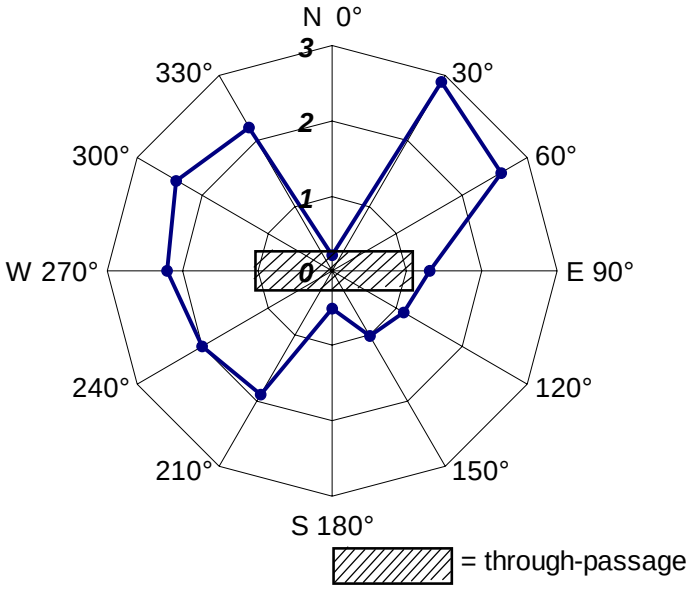
N 0°
3
2
1
0
30°
60°
E 90°
120°
150°
S 180°
210°
240°
W 270°
300°
330°
= through-passage

Figure 7

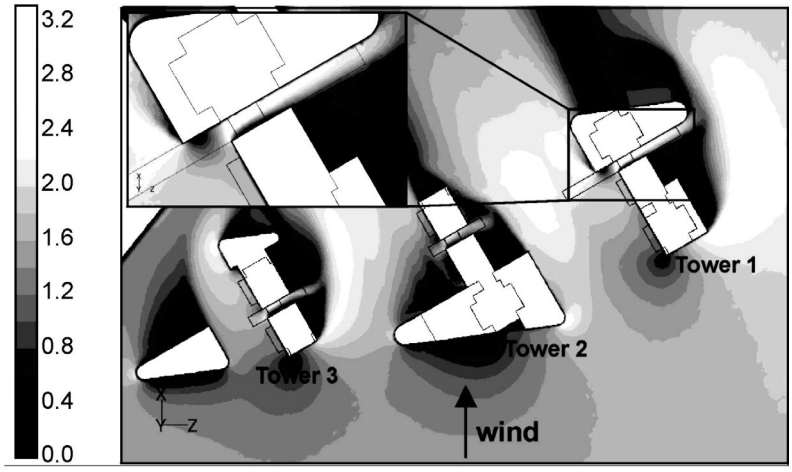

Figure 8a

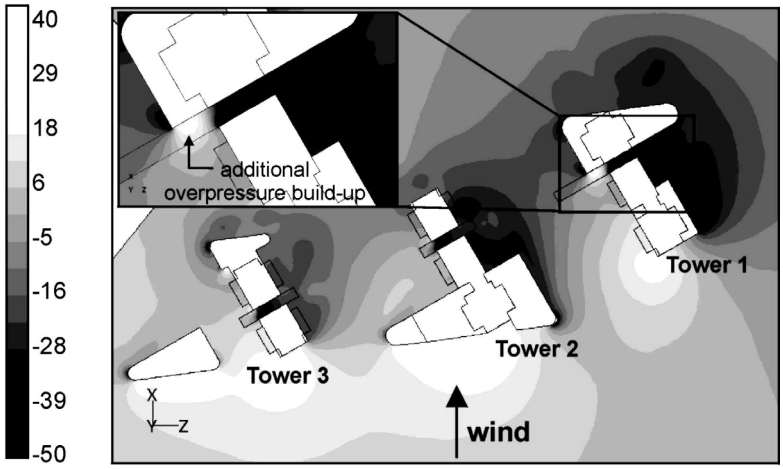

Figure 8b

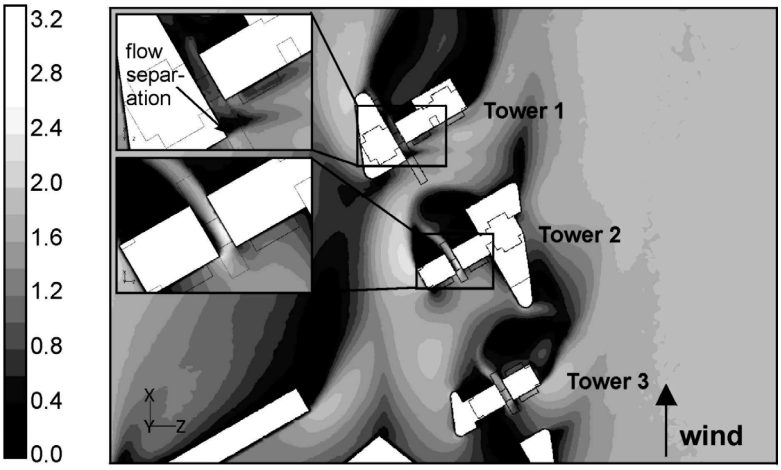
3.2
2.8
2.4
2.0
1.6
1.2
0.8
0.4
0.0
flow
separ-
ation
Tower 1
Tower 2
Tower 3
wind
X
Y
Z

Figure 9

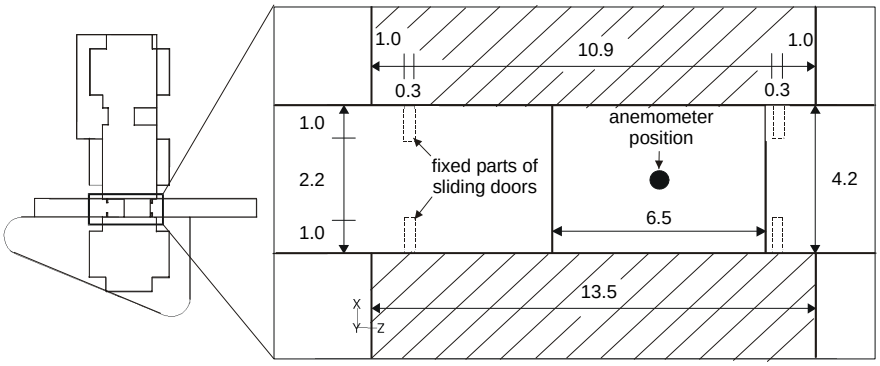
1.0
10.9
1.0
0.3
0.3
1.0
2.2
1.0
fixed parts of
sliding doors
anemometer
position
6.5
4.2
13.5
X
Y
Z

Figure 10

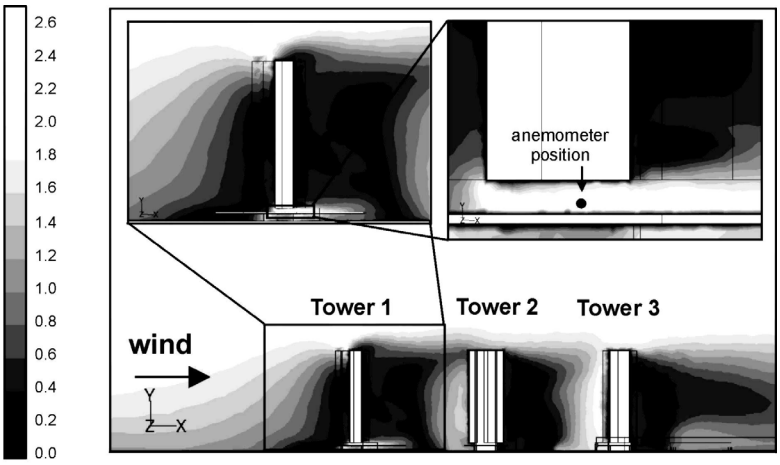
2.6
2.4
2.2
2.0
1.8
1.6
1.4
1.2
1.0
0.8
0.6
0.4
0.2
0.0
anemometer
position
Tower 1
Tower 2
Tower 3
wind
Y
Z
X

Figure 11

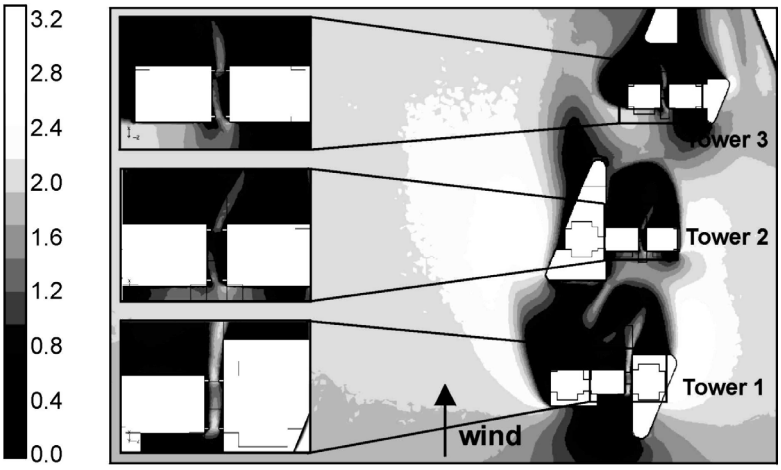

Figure 12a

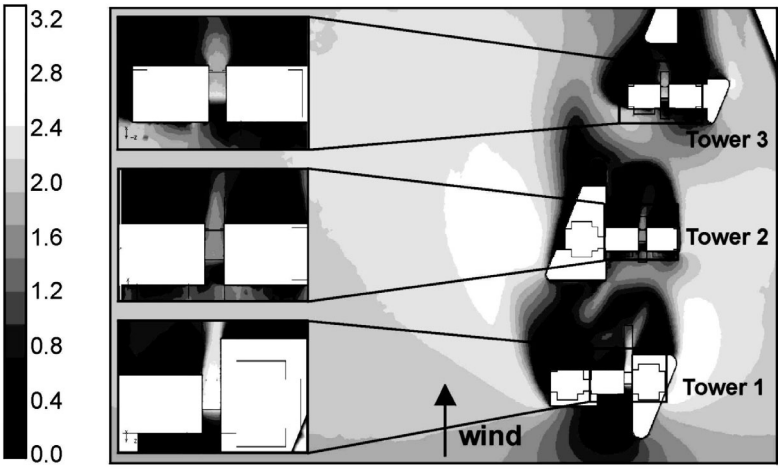

Figure 12b

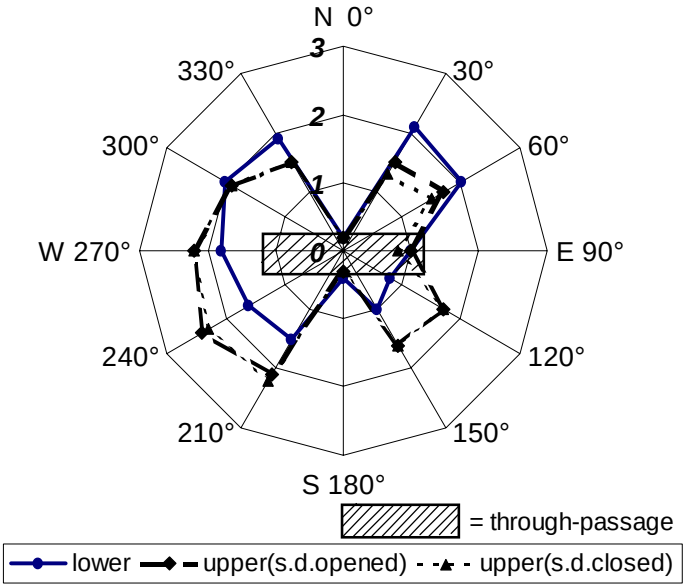
N 0°
30°
60°
E 90°
120°
150°
S 180°
210°
240°
W 270°
300°
330°
3
2
1
0
= through-passage
lower
upper(s.d.opened)
upper(s.d.closed)

Figure 13

FIGURE CAPTIONS

Figure 1 Perspective view of the Silvertop Towers (old design) and the surrounding buildings.

Figure 2 Schematic representation of the link between potential wind speed U_{pot}, wind speed U_{10}, reference wind speed U_0 and local wind speed U. IBL = internal boundary layer.

Figure 3 (a) Site of the Silvertop Towers - new design. The new design comprises passages through towers 1, 2, 3, canopies in the passages, low-rise finlet-shaped buildings at the towers' base and an energy building. South of the towers, an apartment building and a concentration of house blocks exist.
(b) Front view (from west) of tower 1 with detail of through-passage, top view and perspective view of tower 1. The building entrances are situated in the through-passage. A canopy divides the passage into two parts: an upper passage and a lower passage. (Dimensions are given in meter).

Figure 4 Rectangular building and passage geometry. The x-axis traverses the passage along its center line at a height of 2 m (full scale, pedestrian height) above ground.

Figure 5 Comparison of numerical and experimental results in terms of the amplification factor U/U_0. (a) U/U_0 along passage center line and for building dimensions L = 80 m; B = 10 m; H = 6 m; h = 4 m and for varying passage width; (b) same as for figure 5a but with building height H = 18 m; (c) U_M/U_0 (maximum amplification factor in the passage) and for fixed passage width as a function of building height.

Figure 6 Control volume mesh at the west face of tower 1. Local mesh refinement has been applied inside the passage, near the passage entrance and on the canopy faces.

Figure 7 Wind amplification factor U/U_0 in the through-passage of tower 1. The direction of the through-passage is west-east as indicated.

Figure 8 (a) Contours of amplification factor U/U_0 for wind direction 30° in a horizontal plane at 1.75 m height above ground. A detail is given of the conditions in the passage through tower 1, where the highest amplification factor is found;
(b) Contours of static pressure (Pa) for wind direction 30° in a horizontal plane at 1.75 m height above ground. A detail is given of the conditions near and in the passage through tower 1, where an additional overpressure build-up is observed.

Figure 9 Contours of amplification factor U/U_0 for wind direction 120° in a horizontal plane at 1.75 m height above ground. Details are given of the conditions in the passages through towers 1 and 2, where very different amplification factors are found;

Figure 10 Cross-section with a horizontal plane through tower 1 at 4 m height. All dimensions are given in meter. The sliding doors are opened in this figure, yielding a net opening of 2.2 m. The anemometer is positioned in the middle of the upper passage at 0.6 m above the canopy (see also Figure 11).

Figure 11 Contours of amplification factor U/U_0 for wind direction 270° in a vertical plane that is perpendicular to the side face of the towers. The plane cuts through the passage of tower 1 – the sliding doors are opened. The anemometer will be positioned in the middle of the upper passage (see also Figure 10) at 0.6 m above the canopy, where wind speed gradients are low.

Figure 12 (a) Contours of amplification factor U/U_0 for wind direction 270° in a horizontal plane at 1.75 m height above ground. Details are given of the flow conditions in the lower

passages. The influence of the fixed parts of the sliding doors, acting as screens in the passage, is observed;
(b) Same as (a) but now in a horizontal plane at 4 m height above ground. Details are given of the flow conditions in the upper passages. As opposed to the flow in the lower passages, wind speed gradients in the upper passages are quite small.

Figure 13 Wind amplification factor U/U_0 in the passage through tower 1 for three cases: (1) in the lower passage, (2) in the upper passage with sliding doors opened, (3) in the upper passage with sliding doors closed. The direction of the through-passage is west-east as indicated.

Table 1
Basic components of open loop control system to control the sliding doors

Component type	Specification for the current system
Controlled variable	Wind speed in the lower passage
Controlled device	Doors (open – closed)
Setpoint	Threshold value for wind speed in the lower passage
Measured variable	Wind speed in the upper passage
Sensor	Anemometer in the upper passage
Controller	Digital software controller

Table 2
Sliding door control system. Percentage of time that doors are closed instead of opened (P_{co}) and vice versa (P_{oc}) for each wind direction and summed for all wind directions. Correction factors used: $\beta_1 = 0.81$; $\beta_2 = 0.88$; $\beta_3 = 0.76$

Wind direction		0°	30°	60°	90°	120°	150°	180°	210°	240°	270°	300°	330°	Sum
	Tower	N			E			S			W			
P_{co} (%)	1	0.0	0.0	0.0	0.0	1.1	0.5	0.0	1.5	1.9	0.0	0.0	0.0	5.0
	2	0.0	0.0	0.1	0.0	0.0	0.0	0.0	0.0	1.0	0.0	1.7	0.5	3.3
	3	0.0	0.0	0.0	0.0	0.0	0.0	0.0	3.4	0.7	0.1	0.2	0.0	4.3
P_{oc} (%)	1	0.0	3.0	2.5	0.2	0.0	0.0	0.0	0.0	0.0	0.0	1.2	1.6	8.5
	2	0.0	0.4	0.0	0.3	0.4	0.8	0.0	1.2	0.0	0.4	0.0	0.0	3.5
	3	0.0	1.8	0.1	1.0	0.2	0.2	0.0	0.0	0.0	0.0	0.0	0.6	3.8

Table 3
Sliding door control system. Percentage of time that doors are closed (P_c), closed instead of opened (P_{co}) and vice versa (P_{oc}) for 5 cases (different correction factors) and summed for all wind directions. Percentage P_c comprises percentage P_{co}. P_{oc} is the probability of exceedence of the discomfort threshold. WLSM = weighted least squares method, MIC = minimizing imperfect control, W_{oc} and W_{co} are weighting factors.

		Tower 1 % time	Tower 2 % time	Tower 3 % time
Case 1	*β (wind direction dependent)*	*(*)*	*(*)*	*(*)*
	P_c	38.6	36.7	27.0
	P_{co}	0.0	0.0	0.0
	P_{oc} (= % discomfort)	0.0	0.0	0.0
Case 2	*β (WLSM)*	*0.81*	*0.88*	*0.76*
	P_c	35.1	36.5	27.5
	P_{co}	5.0	3.3	4.3
	P_{oc} (= % discomfort)	8.5	3.5	3.8
Case 3	*β (zero discomfort)*	*1.39*	*1.05*	*1.05*
	P_c	60.8	46.6	47.3
	P_{co}	22.2	9.9	20.4
	P_{oc} (= % discomfort)	0.0	0.0	0.0
Case 4	*β (MIC, W_{oc} = 1,W_{co} = 1, $P_{oc} \leq 10\%$)*	*0.76*	*0.94*	*0.75*
	P_c	31.9	40.2	26.8
	P_{co}	3.3	4.8	3.9
	P_{oc} (= % discomfort)	10.0	1.2	4.1
Case 5	*β (MIC, W_{oc} = 2,W_{co} = 1)*	*1.06*	*0.95*	*0.77*
	P_c	49.0	40.7	27.9
	P_{co}	13.2	5.1	4.6
	P_{oc} (= % discomfort)	2.8	1.1	3.6

(*) values are wind direction dependent, no single value used.